https://doi.org/10.48048/tis.2025.9241

Investigation of Pregelatinized Sago Starch-Decanoic Acid Complex by Ultrasonication and its Potential to Stabilize Oil-In-Water Emulsion

Eduard Fransisco Tethool[1,2], Sri Raharjo[1], Yudi Pranoto[1] and Supriyadi Supriyadi[1,*]

[1]Department of Food and Agricultural Product Technology, Faculty of Agricultural Technology, Universitas Gadjah Mada, Yogyakarta 55281, Indonesia
[2]Department of Agricultural Technology, Faculty of Agricultural Technology, Papua University, Manokwari 98314, Indonesia

([*]Corresponding author's e-mail: suprif248@ugm.ac.id)

Received: 29 October 2024, Revised: 26 November 2024, Accepted: 3 December 2024, Published: 30 January 2025

Abstract

Starch-lipid complexes resulting from inclusions between amylose and fatty acid molecules form helical structures with hydrophilic groups on the outer surface and hydrophobic cavities expected to be applied as stabilizers in emulsion systems. Enhancing the inclusion requires pretreatment to promote the development of starch-lipid complexes. Addition pregelatinization of sago starch at several degrees of gelatinization is expected to increase the complexing index (CI) value. The main objective of this research is to investigate the impact of pregelatinization temperature on the establishment of starch-lipid inclusion complexes between sago starch and decanoic acid (DA) using the ultrasonication method and to examine the function of the produced complexes in enhancing the stability of oil-in-water emulsions. Pregelatinization of sago was performed at 65, 70, and 75 °C. The results showed that starch gelatinization at 65 °C (degree of gelatinization (DG) = 26.62 %), 70 °C (DG = 70.21 %), and 75 °C (DG = 100 %) resulted in CI values of 64.18, 61.87, and 49.34 %, respectively, when complexed with DA. The properties of the formed starch-lipid complexes were characterized by increased crystallinity, thermal stability, and decreased viscosity. Using starch-lipid complexes from pregelatinized sago starch (PSS) and DA as emulsion stabilizers can reduce the increase in emulsion viscosity, improve emulsion cream formation, and maintain emulsion stability during 28 days of storage.

Keywords: Pregelatinized, Sago starch, Decanoic acid, Starch-lipid complex, Emulsion

Introduction

An emulsion represents a biphasic system comprising 2 unmixable liquid phases, such as water and oil. Within an emulsion, 1 phase will be dispersed as droplets within the other phase [1]. The permanence of dispersed droplets from 1 liquid phase to intermingle with the other liquid phase is crucial in defining the commercial value of the emulsion [1]. Surfactants or emulsifiers typically sourced from animal products like egg or milk proteins are commonly employed to uphold emulsion stability. Nonetheless, the challenge of using surfactants lies in their susceptibility to temperature alterations in forming layers [2]. Concurrently, the application of these surfactants has the potential to induce issues like foam formation, entrapment of air, biological interactions, and irritation [1]. Consequently, alternative plant-based components like starch are currently utilized as stabilizing agents in emulsions. On the contrary, the intricate molecular structure of starch and the existence of intramolecular interactions hinder natural starch from dissolving effectively in cold water or oil, ultimately diminishing its capacity to stabilize emulsions. Consequently, adjustments to natural starch are imperative to enhance its efficacy in preserving emulsion stability, encompassing measures such as the development of starch-lipid complexes [3-5].

Starch-lipid complexes are produced by developing inclusion complexes formed between amylose molecules and fatty acid compounds. This

interaction causes the amylose molecules to form a helical structure with hydrophilic groups on the outer surface and hydrophobic cavities that bind to the aliphatic chains of fatty acids inside [6,7]. The presence of hydrophilic and hydrophobic parts in the starch-lipid complex is expected to allow the complex to be applied as a stabilizer in emulsion systems.

Ultrasonication is a widely practiced method of forming starch-lipid complexes [8,9]. The characteristics of starch-lipid complexes formed via ultrasonication are significantly influenced by the variety of starch employed in the process [7]. The desired qualities of starch-lipid complexes for their application as emulsion stabilizers include a high degree of crystallinity in type II polymorphic structure, minimal retrogradation tendencies, and relatively small particle size [1,4,110]. One of the starches that meet these characteristics is sago starch (*Metroxylon sago*) [11]. The disadvantage of sago starch is that it has low expandability, solubility, and high retrogradation [12,13], so it needs to be improved by pre-gelatinization.

Pregelatinized starch is starch that has been heated until the granules are damaged and broken and then dried again. Pregelatinized starch can be divided into partially pregelatinized starch and fully pregelatinized starch based on the DG [14,15]. Pregelatinized starch will cause granule breakage, increasing starch solubility and amylose leaching, decreasing viscosity and retrogradation [16,17]. The release of amylose leads to enhanced chances of amylose-fatty acids interactions, thereby promoting the synthesis of starch-lipid complexes [18].

The length of fatty acid chains has an impact on the characteristics of starch-lipid complexes. Fatty acids with shorter chains tend to yield type II polymorphic forms and reduce retrogradation rates, whereas those with longer chains can enhance the hydrophobicity and stability of such complexes [7,19,20]. With a medium chain length, DA forms the most optimal starch-lipid complex when combined with corn starch [9]. Thus, it is expected that during the ultrasonication process, the gelatinization of sago starch will increase the interaction with DA, forming starch-lipid inclusion complexes. Another benefit acquired through the gelatinization of starch is its capability to function as an emulsion stabilizer [21,22]. The starch-lipid complexes produced from PSS and DA are expected to be able to stabilize emulsions.

This research intends to investigate the impact of gelatinization on the creation of starch-lipid inclusion complexes formed by sago starch and DA through ultrasonication and the function of the resultant starch-lipid complexes in stabilizing oil-in-water emulsions.

Materials and methods

Materials

Sago starch (*Metroxylon sago*) was purchased from a local market in Manokwari, West Papua Province, Indonesia. DA was obtained from Sigma Aldrich Corporation. RBD Palm Oil was provided by PT. Bina Karya Prima in Bekasi, Indonesia, and other reagents with analytical grade were used in this study.

Preparation of PSS

The sago starch suspension (1000 mL with a 5 % starch concentration) was subjected to designated thermal conditions (65 ± 1, 70 ± 1, and 75 ± 1 °C) and held at those temperatures for 10 min while continuously stirring (MS-H280pro, DLab, China). Subsequently, the gelatinized starch was cooled to 5 - 10 °C for 3 min, poured into a stainless-steel tray, and dried at 50 °C until it reached a moisture level of around 13 % wb. The PSS was then milled and sieved employing a 100 mesh sieve, classified as PSS 65, PSS 70, and PSS 75, representing sago starch pregelatinized at 65, 70, and 75 °C, respectively. Moreover, Native refers to sago starch that is not subjected to pregelatinization [21].

Preparation of PSS-DA complex by ultrasonication

The preparation of the PSS-DA complex (PSS + DA complex) was referred to Dewi *et al*. [23] and Kang *et al.* [9] with a slight adjustment. Zero point 6 g of DA were solubilized in 40 mL of ethanol and introduced into the PSS solution containing 6 g of PSS within 60 mL of deionized water. The composite was heated to 60 °C with continuous stirring for 30 min. Then, it was ultrasonicated for 15 min using an ultrasonic processor (TF-900N, Tefic Biotech, China) at 50 % ultrasonic amplitude (power density 450 W/cm^2) with pulse intervals every 4 s. The PSS + DA suspension was cooled to room temperature and centrifuged (DM0636, DLab, China) at 1500× g for 15 min. Then, it was

washed with 100 mL of 50 % ethanol and centrifuged at 1500× g for 15 min. Then, the PSS + DA complex dried at 50 °C and ground for analysis. The obtained complexes were then stated as Native + DA, PSS 65 + DA, PSS 70 + DA, and PSS 75 + DA, which indicated that the complexes were made from native sago starch, PSS 65, PSS 70, and PSS 75 with DA, respectively.

Morphology of PSS

Morphology of native and PSS was analyzed utilizing scanning electron microscopy (SEM) (JSM-6510LA, Akishima, Japan). Prior to examination, the specimens were attached to an aluminum stub and covered with a thin film of gold through sputter deposition. Visualization was performed at 500× magnification and an accelerating potential of 5 kV [24].

CI

PSS + DA complexes' CI value was measured using the method outlined by Kang *et al*. [9] and some adjustments. The 2.0 g sample was solubilized in 20 mL of deionized water and subjected to 95 °C for 30 min. A 5.0 g portion of the obtained sample paste was mixed with 25 mL of deionized water. Following agitation with a vortex mixer for 2 min, the sample was centrifugated at 1700× g for 15 min. Subsequently, 500 µL of the resulting supernatant was combined with 15 mL of distilled water and 2 mL of an iodine solution (2.0 % KI and 1.3 % I_2 in deionized water). The sample's absorbance was determined at a wavelength of 690 nm using a spectrophotometer (Genesys 10S, Thermo Scientific, USA). The CI value is calculated by Eq. (1), where the absorbance of native starch is expressed as A*starch* and the absorbance of the PSS + DA complex is expressed as A*complex*.

$$\text{CI (\%)} = \left(\frac{\text{A}starch - \text{A}complex}{\text{A}starch}\right) \times 100 \quad (1)$$

Thermal properties and DG

The thermal characteristics of samples were evaluated utilizing a differential scanning calorimeter (DSC-60 Plus, Shimadzu, Japan). Three point 5 mg of samples was added to 5 µL of distilled water and loaded in a standard aluminium container (an empty container was utilized as a control). The samples were securely sealed and examined across a temperature range of 30 - 100 °C at a heating pace of 10 °C/min. The melting enthalpy (ΔH) was calculated based on the peak endotherm area related to starch gelatinization [25]. The DG was determined using Eq. (2), where Δ*Hns* are the melting enthalpies of native, and Δ*Hts* are treated starches.

$$\text{DG (\%)} = \left(\frac{\Delta H ns - \Delta H ts}{\Delta H ns}\right) \times 100 \quad (2)$$

Fourier-transform infrared (FTIR) spectroscopy

An FTIR spectrophotometer (Thermo Nicolet IS 10, Thermo Fischer Scientific, USA) was employed to collect the FTIR spectra of the PSS-DA complex. Samples weighing 3 mg were analyzed in KBr disks of 300 mg, subjected to scanning within the spectral range of 400 - 4000 cm^{-1}, using a resolution of 8 cm^{-1} [26].

X-ray diffraction

The X-ray diffractometer (Bruker D2, Phaser, Germany) was utilized to analyze the crystalline structure of the PSS + DA complexes. The examination was performed utilizing Cu-Kα radiation (λ = 0.1542 nm) at 40 kV with a scanning range of 2θ from 4 to 35 ° and a speed of 0.02 °/s [9]. The software program Origin Pro (OriginPro 2019, OriginLab Corporation, Northampton, MA, USA) was employed to determine the total area under the curve and the crystalline region (integral of each distinct peak) [24]. The samples' relative crystallinity (RC) was then calculated following the Eq. (3), where A*c* is the crystalline peak area and A*t* is the total area under the curve.

$$\text{RC (\%)} = \left(\frac{\text{A}c}{\text{A}t}\right) \times 100 \quad (3)$$

Pasting properties

The pasting characteristics of native, PSS, and PSS + DA complexes were assessed using a Rapid Visco Analyzer (RVA-4500, Perten Instruments, Sweden) [17]. Three g of the samples were placed and mixed with 25 mL of distilled water inside specific enclosures. The samples were subjected to a thermal cycle from 50 to 95 °C at a heating rate of 6 °C/min, followed by a dwell period at 95 °C for 5 min, then cooled back to 50 °C at the same heating rate, and held at 50 °C for an additional 2 min. The test involved a

paddle rotation at 960 rpm for the first 10 s and 160 rpm for the rest of the experiment. Key parameters monitored include peak viscosity, trough viscosity, breakdown viscosity, final viscosity, and setback viscosity.

Apparent viscosity and emulsion cream stability (ECS)

Oil-in-water emulsions were created following the protocol established by Saw *et al*. [27] with minor adjustment of time and rpm homogenizer. The emulsion is made with water: oil ratio is 8:2. PSS + DA complexes (200 mg per mL oil) were suspended in distilled water and mixed with palm oil. After that, the resulting blend was homogenized using an Ultraturrax homogenizer (T25, IKA, Germany) at 10,000 rpm for 3 min. The emulsion was subsequently placed into a 50 mL centrifuge tube and subjected to centrifugation (DM0636, DLAB, China) at a speed of 3000 rpm for 10 min. The ECS was determined using Eq. (4) at day 0 (fresh condition) and after being stored at ambient temperature (25 ± 1 °C) for 28 days to evaluate changes in emulsion stability.

$$\text{ECS (\%)} = \left(\frac{\text{Height of emulsion layer}}{\text{Total height}}\right) \times 100 \quad (4)$$

The viscosity of the emulsion was determined using a Brookfield viscometer (DV2T model) at room temperature, operating at 30 rpm with spindle number 61.

Statistical analysis

The data obtained is expressed as mean and standard deviation. Statistical analysis was continued with one-way ANOVA at a significance level $p = 0.05$, and later Duncan's post-hoc test was used to evaluate significant differences among the treatments. All data was statistically performed by SPSS (IBM Statistic Version 25, Chicago, USA).

Results and discussion

Morphology of PSS

The shape and appearance of the Native and PSS were examined using scanning electron microscopy (SEM) and illustrated in **Figure 1**. Native sago starch has an oval granule shape (**Figure 1(a)**) which is similar to the granule characteristics of sago starch as previously reported [13,28]. The results of morphological observations showed that when pregelatinized at 65 °C (**Figure 1(b)**) some of the starch granules were gelatinized (marked by yellow arrows), however most of the starch was still in the form of granules or had not been gelatinized. While pregelatinized at 70 °C (**Figure 1(c)**), the starch underwent structural changes which indicated the occurrence of starch gelatinization, but there were still small granules that have not been gelatinized (marked with red arrows). The starch structure was completely changed when pregelatinized at 75 °C (**Figure 1(d)**) which indicates that all the granules have been gelatinized. This is consistent with was previously reported that sago starch has a gelatinization temperature range of 60 - 77 °C [13,24]. Granule damage and structural changes due to the gelatinization process are expected to increase solubility and facilitate the leaching of amylose which increases the ability to form starch-lipid complexes [16,29].

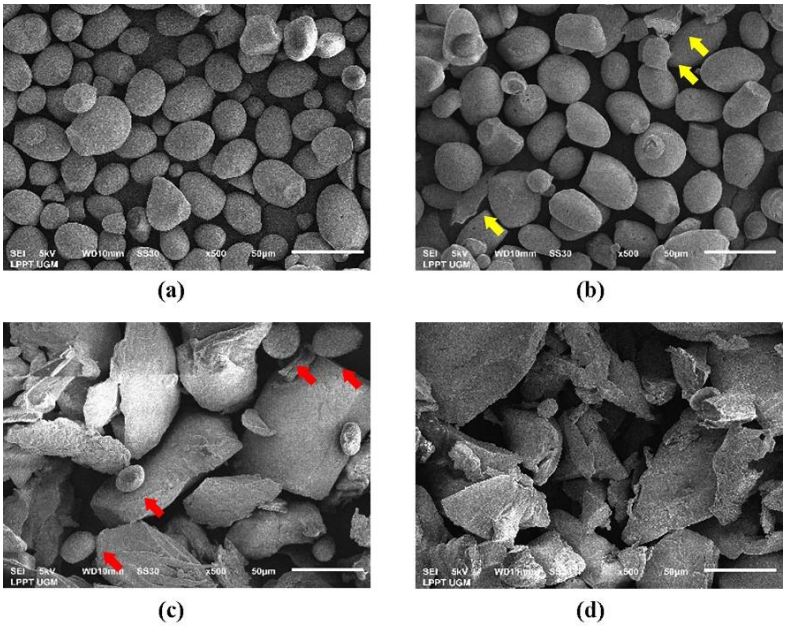

Figure 1 Scanning electron microscopy (SEM) images of native and PSS samples at magnification images of 500×: (a) Native starch, (b) Pregelatinized at 65 ℃ (PSS 65), (c) Pregelatinized at 70 ℃ (PSS 70), and (d) Pregelatinized at 75 ℃ (PSS 75).

DG and CI

The value of the DG indicates the amount of starch that has been gelatinized [15]. The DG of PSS and the CI value of PSS + DA complex are shown in **Figure 2**. The data presented in **Figure 2(a)** illustrates that the sago starch underwent partial gelatinization when subjected to pregelatinization temperatures of 65 and 70 ℃, yielding DG of 26.62 and 70.21 %, respectively. Pregelatinization at 75 ℃ yielded fully gelatinized starch (DG = 100 %). This is influenced by the gelatinization temperature of native sago starch, which ranges from 60 - 77 ℃ [13].

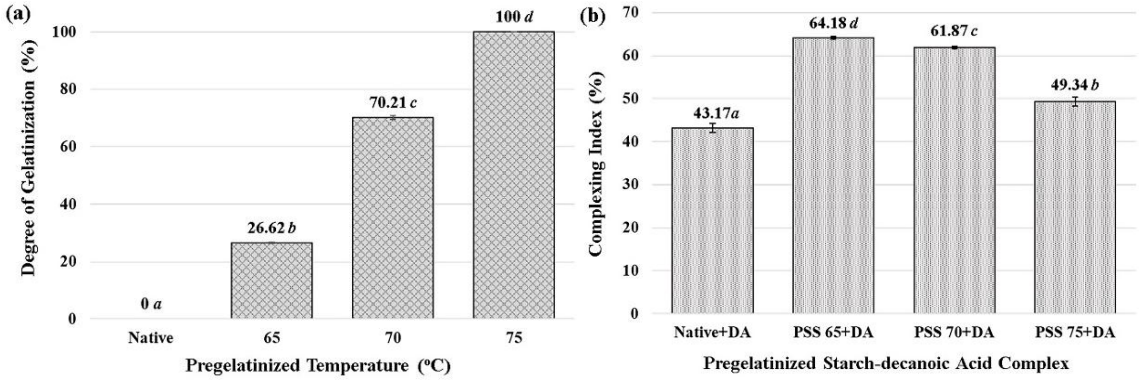

Figure 2 DG and CI: (a) Gelatinization degree of PSS and (b) CI of pregelatinized sago starch-decanoic acid (PSS-DA) complex.

The CI quantifies the complexes resulting from the interaction between amylose molecules in starch and fatty acids [26]. The effect of the pregelatinization of sago starch on the CI value is shown in **Figure 2(b)** pregelatinization at 65, 70, and 75 ℃ resulted in CI values of 64.18, 61.87, and 49.34 %, respectively. There was a rise in these values in comparison to the CI values of starch-lipid complexes developed from Native starch due to the detrimental impact of the gelatinization process on granules, leading to the increased release of amylose and amylopectin into the surrounding medium [21,30]. The release of amylose will enhance its

interaction with DA, forming the amylose-lipid complex [18]. **Figure 2** shows that the higher the pregelatinization temperature and DG reduce the CI value significantly ($p < 0.05$). An optimal level of short-range molecular order is conducive to the maximum formation of complexes, contributing to the decrease in the CI value as the gelatinization degree rises. Below the optimum level, it leads to interference and constrains the movement of starch molecules. Conversely, exceeding the optimal level can result in excessive disorder or entanglement of amylose molecules, diminishing their ability to form complexes with fatty acids [31]. Another factor is that more amylose molecules are released in the pregelatinization process at PSS 70 and PSS 75, and they re-associate to form a crystalline structure during retrogradation (**Figures 1(c) - 1(d)**). This crystalline re-formation decreases the ability of PSS + DA complex formation [32]. While PSS 65 has a lower DG and retrogradation, the ultrasonication process allows for increased granule breakage and thus facilitates the creation of PSS + DA complexes [33,34].

Fourier-transform infrared (FTIR) spectroscopy

FTIR spectroscopy confirmed the alterations in the molecular structure of PSS + DA complexes formed by PSS and DA. **Figure 3** displays a comparative analysis of the FTIR spectra of DA, Native, and PSS + DA complex. DA has an infra red spectrum with characteristic primary absorption at 1707.65, 2855.09 and 2922.59 cm^{-1} bands. The absorption at 1707.65 cm^{-1} indicates the presence of carboxylic groups of DA, as typical carboxylic groups (-COOH) usually show primary absorption in 1705 to 1720 cm^{-1} [35]. While the IR absorption at 2855.09 and 2922.59 cm^{-1} is attributed to the presence of asymmetric stretching vibrations of -CH_3 and -CH groups in fatty acids [36-38]. The FTIR spectrum of native sago starch reveals characteristic absorption peaks, such as a peak at 3420 cm^{-1} corresponding to the hydroxyl (-OH) group within the starch molecule. Additionally, 2924 and 2887.89 cm^{-1} peaks indicate stretching within the carbon-hydrogen (C-H) band. Furthermore, the peak at 1647 cm^{-1} is attributed to the hydroxyl group originating from residual bound water [38,39].

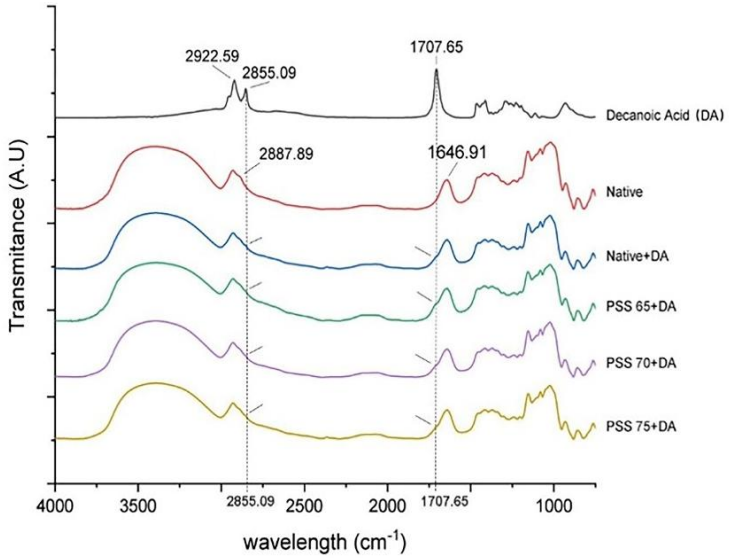

Figure 3 Fourier transform infrared (FTIR) spectrum (wavelength range 750 and 4000 cm^{-1}) of DA, PSS and PSS + DA complex.

FTIR spectra of starch-lipid complexes produced in Native + DA, PSS 65 + DA, PSS 70 + DA, and PSS 75 + DA showed similar absorption characteristics with Native starch, namely in the bands 3420, 2924, 2887.89 and 1647 cm^{-1}. In addition, there are 2 additional absorption peaks, at 1707.65 and 2855.09 cm^{-1}, with increased absorption intensity in the PSS + DA complex compared to Native and PSS, shown in **Table 1**. The presence of the 2 additional absorption bands confirmed that DA added to PSS by ultrasonication successfully

formed starch-lipid inclusion complexes. Previous studies reported that the formation of starch-lipid complexes causes additional IR spectral absorption peaks, which originate from the absorption of the added fatty acid groups. The additional absorption peaks are in the range of 1700 to 1710 cm^{-1} due to the absorption of carboxylic groups and in the range of 2850 to 2857 cm^{-1} due to asymmetric -CH stretching vibrations [20,26,30,37]. **Table 1** shows that in PSS, the absorbance at 1707 and 2855 cm^{-1} is not different from Native starch, indicating no additional absorption peaks. In contrast, the formation of the PSS + DA complex produces additional absorption, where the highest absorption peak is obtained at the PSS 65 + DA complex. This absorbance is influenced by the amount of starch-lipid complex formed, which the CI value indicates (**Figure 2(b)**). The higher the CI value of the starch-lipid complex, the higher the absorption peak obtained (**Table 1**).

Table 1 Structural parameters of PSS and PSS + DA complex.

	FTIR absorbance (intensity)		Helix structure (intensity)		Relative crystallinity (%)
	1707.65	2855.09	995/1022 ratio	1083	
Native	63.51 ± 0.165^{ab}	73.58 ± 0.230^{b}	0.839 ± 0.0095^{d}	31.23 ± 0.35^{a}	30.66 ± 0.79^{d}
PSS 65	63.76 ± 0.281^{b}	73.42 ± 0.276^{ab}	0.723 ± 0.0509^{a}	34.24 ± 0.56^{c}	28.16 ± 0.50^{c}
PSS 70	63.44 ± 0.301^{ab}	73.04 ± 0.297^{a}	0.749 ± 0.0222^{ab}	32.76 ± 0.66^{b}	26.47 ± 1.29^{b}
PSS 75	63.21 ± 0.331^{a}	73.32 ± 0.192^{ab}	0.784 ± 0.0112^{bc}	31.58 ± 0.46^{a}	14.71 ± 0.16^{a}
Native + DA	70.26 ± 0.363^{c}	75.16 ± 0.226^{c}	0.822 ± 0.0064^{cd}	38.47 ± 0.49^{d}	31.02 ± 0.13^{de}
PSS 65 + DA	76.41 ± 0.149^{f}	77.25 ± 0.188^{f}	0.736 ± 0.0085^{ab}	52.81 ± 0.29^{f}	36.76 ± 0.63^{g}
PSS 70 + DA	75.83 ± 0.208^{e}	76.67 ± 0.199^{e}	0.783 ± 0.0099^{bc}	46.59 ± 0.59^{e}	34.73 ± 0.84^{f}
PSS 75 + DA	73.11 ± 0.287^{d}	75.83 ± 0.219^{d}	0.815 ± 0.0063^{cd}	47.22 ± 0.35^{e}	32.55 ± 0.06^{e}

Note: Results are presented as mean ± SD; superscripts indicate significant difference ($p < 0.05$) in the column. 995/1022 ratio indicates intensity of amylose double helix; 1083 indicates intensity of amylose single helix.

The crystallographic configuration and immediate alignment of starch can be assessed by utilizing infrared spectra within the 800 - 1200 cm^{-1} peak range [24,37]. The frequencies at 850 and 928 cm^{-1} correspond to the vibrational modes of the side chain ramifications in amylopectin, whereas the peak at 991 cm^{-1} reflects the level of double helix structure in amylopectin [40]. The intensity ratio of the peak spectra at 995 to 1022 cm^{-1} measures the level of double helix formation in amylose, with the peak at 1083 cm^{-1} corresponding to the vibrational mode of the amylose single helix [40]. The data in **Table 1** indicates that Native starch exhibits an elevated level of amylose double helix compared to the starch-lipid complex derived from PSS. This discrepancy can be attributed to the inherent configuration of the amylose molecule that favours the formation of a double helix structure. The disruption of this double helix structure during the pregelatinization process occurs due to the liberation of amylose molecules [30,41]. PSS + DA complex displaying increased DG levels exhibit elevated double helix content. The increase is because more amylose molecules are released in the gelatinization process and, during retrogradation, will re-associate to form a double helix [32]. Due to retrogradation, the presence of amylose double helix will reduce the ability of starch-lipid complex formation, characterized by the decrease of amylose single helix degree in PSS + DA complex formation (**Table 1**). This condition caused the starch gelatinization treatment at 65 °C with a 26 % gelatinization degree, resulting in the highest CI value (**Figure 2(b)**).

X-ray diffraction

Starch can be classified based on the crystalline structure pattern by X-ray diffraction (XRD). A-type of crystalline structure has 2θ diffraction peaks at 15, 17, 20, and 23 °; B-type at 5, 17, 20, 22, and 24 °; C-type is the result of the merging of characteristics from both A-type and B-type; while V-type crystalline structure has

2θ diffraction peaks at 7, 13, and 20 ° [9,18,23,42]. The XRD patterns of Native, PSS and PSS + DA complexes formed are illustrated in **Figure 4**, with the corresponding RC values provided in **Table 1**. The diffraction patterns of Native and partially gelatinized sago starch (PSS 65 and PSS 70) showed that sago starch has a C-type crystal form with 2θ diffraction peaks at 10.13, 11.32, 15.12, 17.15, 18.07, 23.15, and 26.28 °, related with the previous studies [13,23,43]. The pregelatinisation process does not alter the crystal structure of starch but progressively reduces the intensity of its crystalline peaks [14,17]. **Figure 4** shows that PSS 75, which has been fully gelatinized, has almost lost the entire C-type crystalline pattern. It is indicated by the decrease of 2θ diffraction peaks at 15.12, 17.15, and 23.15 °, and the peaks at 10.13, 11.32, 18.07 and 26.28 ° have disappeared. Starch gelatinization has converted most crystalline forms into amorphous ones [14,44]. The transition from an ordered crystalline arrangement to a disordered amorphous structure following gelatinization led to a reduction in the level of RC (**Table 1**), as reported in previous studies [17,37,44]. Native sago starch has a RC of 30.66 %, with pregelatinization treatment decreased to 28.16 % (PSS 65), 26.47 % (PSS 70), and 14.71 % (PSS 75).

X-ray diffraction is also capable of detecting the occurrence of starch-lipid complexes [10,23]. **Figure 4** shows that the C-type crystal structure of Native and PSS has transitioned to V-type due to complex formation with DA. This change is characterized by the presence of 2θ diffraction peaks at 7.44, 12.92, 19.84, and 22.46 ° in Native + DA, PSS 65 + DA, PSS 70 + DA, and PSS 75 + DA. PSS for starch-lipid complex formation increased crystallinity compared to Native (**Table 1**). Starch pregelatinization will provide more free amylose molecules to interact with fatty acids [18]. **Table 1** showed that the highest crystallinity was possessed by PSS 65 at 36.76 % and decreased as the DG increased. The crystallinity aligns with the findings of the CI value, which is related to the retrogradation process that occurs during gelatinization. Crystallinity is related to emulsion stability. Thus, PSS + DA complexes with high crystallinity are expected to provide good emulsion stability.

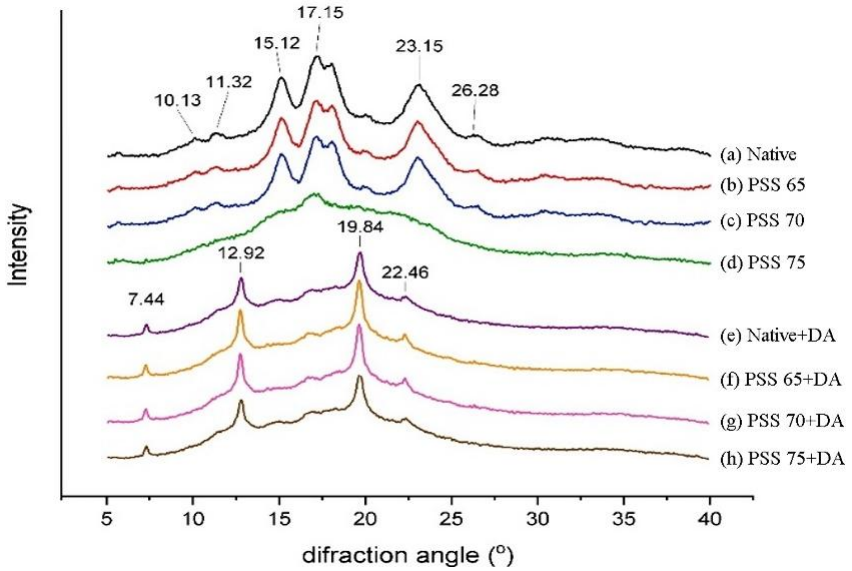

Figure 4 X-ray diffraction patterns of native, PSS and PSS + DA complex: (a) Native, (b) PSS 65, (c) PSS 70, (d) PSS 75, (e) Native + DA, (f) PSS 65 + DA, (g) PSS 70 + DA, and (h) PSS 75 + DA.

Thermal properties

The thermal characteristics of the Native, PSS, and PSS + DA complexes were evaluated through differential scanning calorimeter (DSC), as presented in **Table 2**. DSC parameters on the thermogram describe the energy transition due to the melting or formation of the resulting structure [45]. The partial gelatinization of sago starch (PSS 65 and PSS 70) tended not to change the transition temperature compared to Native but significantly ($p < 0.05$) decreased the enthalpy of gelatinization. This result is similar to what has been reported for cassava and corn starch [14,46]. The

endothermic peak depicted in Native, PSS 65 and PSS 70 (**Table 2**) is the energy required for starch gelatinization [9]. In PSS 75, because the entire starch has been gelatinized (DG = 100 %), there is no more energy uptake of energy needed for gelatinization. This condition is consistent with that reported for corn starch [14]. Meanwhile, the starch-lipid complexes in the Native + DA, PSS 65 + DA, PSS 70 + DA and PSS 75 + DA samples formed endothermic curves depicting fatty acid digestion. **Table 2** shows that the PSS + DA complexes produced have Tp between 148.73 - 168.62 °C. Based on the melting temperature, the PSS + DA complex has a type II polymorph form with melting temperatures above 110 °C [7,47]. Because it has a high melting point, starch-lipid complexes with type II polymorph are more stable to temperature changes [7].

Table 2 Thermal properties of PSS and PSS + DA complex.

	To (°C)	Tp (°C)	Te (°C)	Te-To (°C)	ΔH (J/g)
Native	72.74 ± 0.01^{b}	76.84 ± 0.04^{b}	80.38 ± 0.08^{b}	7.64 ± 0.10^{b}	11.82 ± 0.02^{d}
PSS 65	74.60 ± 0.03^{b}	77.35 ± 0.05^{b}	84.01 ± 0.06^{c}	9.41 ± 0.09^{b}	8.67 ± 0.03^{c}
PSS 70	75.37 ± 0.06^{b}	77.41 ± 0.06^{b}	83.53 ± 0.06^{c}	8.16 ± 0.12^{bc}	4.62 ± 0.08^{b}
bPSS 75	0.00 ± 0.00^{a}	0.00 ± 0.00^{a}	0.00 ± 0.00^{a}	0.00 ± 0.00^{a}	0.00 ± 0.00^{a}
Native + DA	135.11 ± 2.36^{c}	155.58 ± 0.98^{d}	163.82 ± 1.33^{e}	28.71 ± 1.03^{e}	4380.75 ± 0.85^{e}
PSS 65 + DA	159.43 ± 1.49^{e}	168.62 ± 2.26^{f}	172.55 ± 1.01^{f}	13.12 ± 2.50^{cd}	6850.16 ± 1.30^{h}
PSS 70 + DA	154.87 ± 1.97^{d}	165.44 ± 1.21^{e}	171.23 ± 1.25^{f}	16.36 ± 0.71^{d}	6250.24 ± 1.13^{g}
PSS 75 + DA	137.55 ± 3.09^{c}	148.73 ± 1.55^{c}	145.54 ± 1.07^{d}	7.99 ± 4.16^{b}	5870.57 ± 0.77^{f}

Note: Results are presented as mean ± SD; superscripts indicate significant difference ($p < 0.05$) in the column. To: Onset temperature, Tp: Peak temperature, Te: End-set temperature, Te-To: Gelatinization temperature range, and ΔH: Enthalpy.

Thermal properties are closely related to the crystallinity structure. The increase in amylose-fatty acid interaction leads to higher To, Tp, and Te values for starch-lipid complexes, which correlates with increased crystallinity. Consequently, the physical modification of starch leads to an elevated temperature requirement for its gelatinization, causing the disruption of the starch's crystalline structure and raising its transition temperature [23,47]. The range of gelatinization (Te-To) reflects the diversity of crystals within starch granules. A narrow Te-To implies well-formed crystals, whereas a broader range suggests merging crystals with varied stability [48]. In this study, the PSS + DA complex displayed higher enthalpy (ΔH) than Native and PSS, indicating its crystalline enhancement and thermal stability. This observation aligns with the RC information obtained from X-ray diffraction analysis (**Table 1**).

Pasting properties of PSS and PSS-DA complex

The paste viscosities of Native, PSS, and PSS + DA complexes are graphically represented in **Figure 5**. The findings indicate a positive correlation between the extent of DG of sago starch and the peak viscosity of the paste. Native starch has a peak viscosity of 4.375 cp, increasing to 9.417 cp in PSS 75, which has been fully gelatinized. This is because the breakdown of granule structure due to gelatinization facilitates the absorption of water molecules into the amorphous part and increases viscosity [16]. At the same time, the creation of the PSS + DA complex often leads to a reduction in viscosity (**Figure 5**). This decline is attributed to the formation of complexes between starch and lipid, resulting in a helix structure that inhibits water absorption [16,17]. Previous studies reported that CI affected viscosity, and the higher the CI value, the marked decrease in breakdown and setback viscosity [37,48]. This condition is due to the complex formation with stable type-II polymorph increases so that a more organized crystal structure can maintain the thermal stability of starch paste [7].

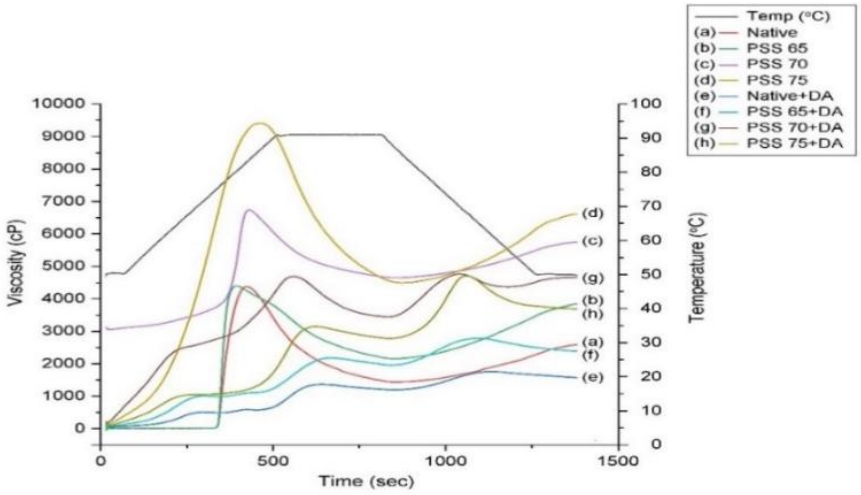

Figure 5 Pasting properties of PSS and PSS-DA complex: (a) Native, (b) PSS 65, (c) PSS 70, (d) PSS 75, (e) Native + DA, (f) PSS 65 + DA, (g) PSS 70 + DA, and (h) PSS 75 + DA.

Apparent viscosity and ECS

The results of emulsion viscosity measurements under fresh conditions (0 days) and after 28 days of storage are outlined in **Table 3**. Emulsions made with PSS exhibited significantly higher viscosity ($p < 0.05$) than those produced with PSS + DA complexes. Increasing the DG of starch augmented the viscosity of the resulting emulsion due to the superior water absorption capacity of pregelatinized starch [22]. Emulsion viscosity is closely linked to the properties of PSS + DA complex paste, as illustrated in **Figure 5**. The formation of PSS + DA complexes can reduce peak and setback viscosity compared to PSS [37,48], reducing the overall emulsion viscosity. **Table 3** indicates that after 28 days of storage, the emulsion which used Native as a stabilizer was compromised and could not be measured (for viscosity and ECS), while the viscosity of other emulsions tended to decline. The damage of this emulsion is primarily attributed to dispersed phase droplets' deflocculation and emulsion constituents' breakdown [22]. **Table 3** shows that the utilization of PSS + DA complexes can maintain the decrease in emulsion viscosity during storage, demonstrated by the lack of a significant reduction ($p > 0.05$) in viscosity after 28 days ($p > 0.05$). The ability to maintain emulsion viscosity is attributed to the more resilient structure of the starch-lipid complex, which aids in sustaining the emulsion system [3,4].

Table 3 Characteristics of emulsions stabilized by PSS-DA complex.

	Viscosity (cp)		**Emulsion cream stability (%)**	
	Fresh (0 days)	**After 28 days**	**Fresh (0 days)**	**After 28 days**
Native	71.25 ± 1.77^{a}	nd	4.74 ± 0.336^{a}	nd
PSS 65	78.75 ± 0.35^{bB}	75.25 ± 1.06^{cA}	8.28 ± 0.502^{bB}	4.70 ± 0.820^{aA}
PSS 70	84.25 ± 1.77^{cB}	79.50 ± 1.41^{dA}	12.69 ± 1.487^{cB}	7.08 ± 0.339^{bA}
PSS 75	90.00 ± 2.12^{dB}	84.50 ± 1.41^{eA}	14.56 ± 1.199^{cB}	10.011 ± 1.054^{cA}
Native + DA	70.25 ± 1.06^{aB}	65.25 ± 1.77^{aA}	12.97 ± 1.365^{cB}	9.01 ± 1.230^{bcA}
PSS 65 + DA	69.50 ± 2.83^{aA}	67.75 ± 3.89^{abA}	35.60 ± 1.551^{fA}	33.05 ± 0.642^{fA}
PSS 70 + DA	$75.75 \pm 1.06^{b\,A}$	72.50 ± 2.83^{bcA}	32.50 ± 1.013^{eA}	30.68 ± 0.871^{eA}
PSS 75 + DA	78.25 ± 1.06^{bA}	75.25 ± 1.77^{cA}	29.12 ± 2.007^{dB}	27.40 ± 1.278^{dA}

Note: Results are presented as mean ± SD. Lowercase superscripts within the same column indicate a significant difference ($p < 0.05$) determined by ANOVA and Duncan's test, while uppercase superscripts indicate significant differences ($p < 0.05$) determined by t-tests for viscosity and ECS at both 0 and 28 days.

Table 3 shows the emulsion cream formation (0 days) and stability during 28 days of storage. The use of PSS significantly increased the formation of emulsion cream ($p < 0.05$), as has been reported in previous studies [21,22]. In this research, emulsion cream derived from PSS exhibited lower efficacy than the starch-lipid complex. The most favourable emulsion cream formation was observed with PSS 65 + DA, achieving a 35.60 % formation rate, surpassing Native + DA at 12.97 %. This outcome suggests that using a PSS + DA complex notably increased the formation of emulsion cream (0 days). This phenomenon is associated with the CI value, as shown in **Figure 2**. A higher CI value correlates with increased emulsion cream formation. Such enhancement in emulsion cream formation by the PSS + DA complex is caused by the interaction of the hydrophobic tails of fatty acids and amylose, resulting in the hydrophobic helical cavity that facilitates the entrapment of oil within the emulsion cream [6,49,50].

The ECS was evaluated after being stored at ambient conditions for 28 days. Emulsions exhibit inherent instability due to their thermodynamics, making them susceptible to phase separation and evolving with time. One of the factors influencing ECS is the interfacial tension, which can be managed by incorporating surfactants or other additives [50]. A decline in emulsion cream was observed throughout the storage period compared to the initial state (0 days). **Table 3** exhibits a notable reduction in cream stability ($p < 0.05$) in emulsions which use PSS as a stabilizer. Conversely, a non-significant decrease in ECS ($p > 0.05$) was observed using a PSS + DA complex. The application of the PSS 65 + DA complex to preserve ECS, the ECS decreased from 35.60 to 33.05 %, showing no significant difference ($p > 0.05$). Previous research reported that emulsions using corn starch-propionate were stable for 14 days of storage [4], while the use of granular cold water swelling maize starches was reported to maintain emulsion stability for up to 21 days of storage [22]. In addition, pregelatinized waxy rice starch can maintain emulsion stability for up to 21 days of storage [21]. The efficacy of some modified starches in maintaining emulsion stability during storage is influenced by increasing the yield stress and viscosity of the emulsion. The ability to hold the ECS suggests that utilizing PSS + DA complexes helps preserve emulsion stability by absorbing oil droplets and creating an interfacial layer in o/w emulsions that inhibits the aggregation of oil droplets [3,4].

Conclusions

The formation of the starch-lipid complex from PSS and DA resulted in the highest complex index in sago starch gelatinized at 65 °C with a gelatinization degree of 26.62 %. The higher temperature and degree of gelatinase reduced the CI of the starch-lipid complex. FTIR analysis and the change of crystalline pattern to V-type confirmed the formation of the starch-lipid complex. The characteristics of the resulting starch-lipid complexes were characterized by increased crystallinity, thermal stability, and decreased viscosity. Using starch-lipid complexes from PSS and DA as emulsion stabilizers can reduce the increase in emulsion viscosity, improve emulsion cream formation, and maintain emulsion stability during 28-day storage.

Acknowledgements

The authors wish to acknowledge the support provided by the Indonesian Endowment Fund for Education (LPDP Indonesia) and the Ministry of Finance of the Republic of Indonesia under the reference number: KET-1603/LPDP.4/2019.

References

[1] F Zhu. Starch based Pickering emulsions: Fabrication, properties, and applications. *Trends in Food Science & Technology* 2019; **85**, 129-137.

[2] M Destribats, S Gineste, E Laurichesse, H Tanner, F Leal-Calderon, V Héroguez and V Schmitt. Pickering emulsions: What are the main parameters determining the emulsion type and interfacial properties? *Langmuir* 2014; **30(31)**, 9313-9326.

[3] LF Hong, LH Cheng, CY Lee and KK Peh. Characterisation of physicochemical properties of propionylated corn starch and its application as stabilizer. *Food Technology and Biotechnology* 2015; **53(3)**, 278-285.

[4] LF Hong, LH Cheng, CY Gan, CY Lee and KK Peh. Evaluation of starch propionate as emulsion stabiliser in comparison with octenylsuccinate

starch. *LWT - Food Science and Technology* 2018; **91**, 526-531.

[5] X Lu, H Liu and Q Huang. Fabrication and characterization of resistant starch stabilized Pickering emulsions. *Food Hydrocolloids* 2020; **103**, 105703.

[6] T Feng, H Zhuang, F Chen, O Campanella, D Bhotpakar, MA Carignano and SH Park. *Starch-lipid and starch-protein complexes and their application. In*: Z Jin (Ed.). Functional starch and applications in food. Springer Singapore, 2018, p. 177-226.

[7] S Wang, C Chao, J Cai, B Niu, L Copeland and S Wang. Starch-lipid and starch-lipid-protein complexes: A comprehensive review. *Comprehensive Reviews in Food Science and Food Safety* 2020; **19(3)**, 1056-1079.

[8] P Liu, R Wang, X Kang, B Cui and B Yu. Effects of ultrasonic treatment on amylose-lipid complex formation and properties of sweet potato starch-based films. *Ultrasonics Sonochemistry* 2018; **44**, 215-222.

[9] X Kang, P Liu, W Gao, Z Wu, B Yu, R Wang, B Cui, L Qiu and C Sun. Preparation of starch-lipid complex by ultrasonication and its film forming capacity. *Food Hydrocolloids* 2020; **99**, 105340.

[10] MC Garcia, MA Pereira-Da-Silva, S Taboga and CML Franco. Structural characterization of complexes prepared with glycerol monoestearate and maize starches with different amylose contents. *Carbohydrate Polymers* 2016; **148**, 371-379.

[11] H Ehara, DV Johnson and Y Toyoda. *Sago palm: Multiple contributions to food security and sustainable livelihoods*. Springer Nature, Cham, Switzerland, 2018.

[12] EF Tethool, A Jading and B Santoso. Characterization of physicochemical and baking expansion properties of oxidized sago starch using hydrogen peroxide and sodium hypochlorite catalyzed by UV irradiation. *Food Science and Quality Management* 2012; **10(1)**, 1-11.

[13] B Santoso, K Sakakura, H Naito, M Ohmi, Y Nishimura, T Uchiyama, A Itaya, M Hisamatsu, H Ehara and T Mishima. Effects of wet milling sago pith waste on yield and physical properties of sago starch. *International Journal of Engineering & Technology* 2017; **17(2)**, 1-6.

[14] ZQ Fu, LJ Wang, D Li and B Adhikari. Effects of partial gelatinization on structure and thermal properties of corn starch after spray drying. *Carbohydrate Polymers* 2012; **88(4)**, 1319-1325.

[15] TPRD Santos, CML Franco, IM Demiate, XH Li, EL Garcia, JL Jane and M Leonel. Spray-drying and extrusion processes: Effects on morphology and physicochemical characteristics of starches isolated from Peruvian carrot and cassava. *International Journal of Biological Macromolecules* 2018; **118**, 1346-1353.

[16] M Majzoobi, Z Kaveh and A Farahnaky. Effect of acetic acid on physical properties of pregelatinized wheat and corn starch gels. *Food Chemistry* 2016; **196**, 720-725.

[17] Y Liu, J Chen, S Luo, C Li, J Ye, C Liu and RG Gilbert. Physicochemical and structural properties of pregelatinized starch prepared by improved extrusion cooking technology. *Carbohydrate Polymers* 2017; **175**, 265-272.

[18] R Wang, P Liu, B Cui, X Kang and B Yu. Effects of different treatment methods on properties of potato starch-lauric acid complex and potato starch-based films. *International Journal of Biological Macromolecules* 2019; **124**, 34-40.

[19] TR Seo, JY Kim and ST Lim. Preparation and characterization of crystalline complexes between amylose and C18 fatty acids. *LWT - Food Science and Technology* 2015; **64(2)**, 889-897.

[20] M Zheng, C Chao, J Yu, L Copeland, S Wang and S Wang. Effects of chain length and degree of unsaturation of fatty acids on structure and *in vitro* digestibility of starch-protein-fatty acid complexes. *Journal of Agricultural and Food Chemistry* 2018; **66(8)**, 1872-1880.

[21] R Yulianingsih and S Gohtani. Dispersion characteristics of pregelatinized waxy rice starch and its performance as an emulsifier for oil-in-water emulsions: Effect of gelatinization temperature and starch concentration. *Food Hydrocolloids* 2019; **95**, 476-486.

[22] S Hedayati, F Shahidi, A Koocheki, A Farahnaky and M Majzoobi. Influence of pregelatinized and granular cold water swelling maize starches on stability and physicochemical properties of low fat

oil-in-water emulsions. *Food Hydrocolloids* 2020; **102**, 105620.

[23] AMP Dewi, U Santoso, Y Pranoto and DW Marseno. Dual modification of sago starch via heat moisture treatment and octenyl succinylation to improve starch hydrophobicity. *Polymers* 2022; **14(6)**, 1086.

[24] Z Liu, C Wang, X Liao and Q Shen. Measurement and comparison of multi-scale structure in heat and pressure treated corn starch granule under the same degree of gelatinization. *Food Hydrocolloids* 2020; **108**, 106081.

[25] L Wang, W Wang, Y Wang, G Xiong, X Mei, W Wu, A Ding, X Li, Y Qiao and L Liao. Effects of fatty acid chain length on properties of potato starch-fatty acid complexes under partially gelatinization. *International Journal of Food Properties* 2018; **21(1)**, 2121-2134.

[26] SS Saw, NY Shariffa, AS Ruri and U Uthumporn. Physicochemical and emulsifying properties of pre-treated octenyl succinic anhydride (OSA) sago starch in simple emulsion system. *Food Research* 2020; **4(4)**, 1326-1332.

[27] F Zhu. Recent advances in modifications and applications of sago starch. *Food Hydrocolloids* 2019; **96**, 412-423.

[28] V Derycke, GE Vandeputte, R Vermeylen, WD Man, B Goderis, MHJ Koch and JA Delcour. Starch gelatinization and amylose-lipid interactions during rice parboiling investigated by temperature resolved wide angle X-ray scattering and differential scanning calorimetry. *Journal of Cereal Science* 2005; **42(3)**, 334-343.

[29] X Lin, X Zhang, B Du and B Xu. Morphological, structural, thermal, pasting, and digestive properties of starches isolated from different varieties of rice: A systematic comparative study. *Foods* 2023; **12(24)**, 4492.

[30] C Chao, S Huang, J Yu, L Copeland, Y Yang and S Wang. The influence of short-range molecular order in gelatinized starch on the formation of starch-lauric acid complexes. *International Journal of Biological Macromolecules* 2024; **260**, 129526.

[31] SC Alcázar-Alay and MAA Meireles. Physicochemical properties, modifications and applications of starches from different botanical sources. *Food Science and Technology* 2015; **35(2)**, 215-236.

[32] W Yang, X Kong, Y Zheng, W Sun, S Chen, D Liu, H Zhang, H Fang, J Tian and X Ye. Controlled ultrasound treatments modify the morphology and physical properties of rice starch rather than the fine structure. *Ultrasonics Sonochemistry* 2019; **59**, 104709.

[33] W Qin, H Xi, A Wang, X Gong, Z Chen, Y He, L Wang, L Liu, F Wang and L Tong. Ultrasound treatment enhanced semidry-milled rice flour properties and gluten-free rice bread quality. *Molecules* 2022; **27(17)**, 5403.

[34] J Han, MSM Annuar, MFK Ariffin, AM Gumel, S Ibrahim, T Heidelberg, B Bakar, ABMS Hossain and Y Sharifuddin. Lipase-catalyzed synthesis of 6-O-D-glucosyldecanoate in tert-butanol: Reaction optimization and effect of mixing power input. *Biotechnology & Biotechnological Equipment* 2011; **25(4)**, 2642-2651.

[35] H Wang, Y Wu, N Wang, L Yang and Y Zhou. Effect of water content of high-amylose corn starch and glutinous rice starch combined with lipids on formation of starch-lipid complexes during deep-fat frying. *Food Chemistry* 2019; **278**, 515-522.

[36] B Chen, S Zeng, H Zeng, Z Guo, Y Zhang and B Zheng. Properties of lotus seed starch-glycerin monostearin complexes formed by high pressure homogenization. *Food Chemistry* 2017; **226**, 119-127.

[37] AMP Dewi, U Santoso, Y Pranoto and DW Marseno. Optimizing reaction condition of octenyl succinic anhydride on heat-moisture-treated sago starch and its application for biodegradable film. *Food Science and Technology* 2023; **43**, e17523.

[38] AB Salim, SF Chin and SC Pang. Hydroxypropyl starch nanoparticles as controlled release nanocarriers for piperine. *Journal of Nanostructures* 2020; **10(2)**, 327-336.

[39] Y Zheng, B Wang, Z Guo, Y Zhang, B Zheng, S Zeng and H Zeng. Properties of lotus seed starch-glycerin monostearin V-complexes after long-term retrogradation. *Food Chemistry* 2020; **311**, 125887.

[40] JA Putseys, LJ Derde, L Lamberts, E Östman, IM Björck and JA Delcour. Functionality of short

chain amylose-lipid complexes in starch-water systems and their impact on *in vitro* starch degradation. *Journal of Agricultural and Food Chemistry* 2010; **58(3)**, 1939-1945.

[41] X Lian, K Cheng, D Wang, W Zhu and X Wang. Analysis of crystals of retrograded starch with sharp X-ray diffraction peaks made by recrystallization of amylose and amylopectin. *International Journal of Food Properties* 2018; **20(S3)**, S3224-S3236.

[42] B Santoso, ZL Sarungallo and AM Puspita. Physicochemical and functional properties of spineless, short-spines, and long-spines sago starch. *Biodiversitas* 2021; **22(1)**, 137-143.

[43] HT Tô, SJ Karrila, LH Nga and TT Karrila. Effect of blending and pregelatinizing order on properties of pregelatinized starch from rice and cassava. *Food Research* 2020; **4(1)**, 102-112.

[44] S Wang, C Li, L Copeland, Q Niu and S Wang. Starch retrogradation: A comprehensive review. *Comprehensive Reviews in Food Science and Food Safety* 2015; **14(5)**, 568-585.

[45] VM Torrejon, H Song, B Wu, G Luo and J Song. Effect of starch type and pre-treatment on the properties of gelatin-starch foams produced by mechanical foaming. *Polymers* 2023; **15(7)**, 1775.

[46] B Goderis, JA Putseys, CJ Gommes, GM Bosmans and JA Delcour. The structure and thermal stability of amylose-lipid complexes: A case study on amylose-glycerol monostearate. *Crystal Growth & Design* 2014; **14(7)**, 3221-3233.

[47] C Chao, J Yu, S Wang, L Copeland and S Wang. Mechanisms underlying the formation of complexes between maize starch and lipids. *Journal of Agricultural and Food Chemistry* 2018; **66(1)**, 272-278.

[48] S Sang, X Xu, X Zhu and G Narsimhan. Complexation of 26-Mer amylose with egg yolk lipids with different numbers of tails using a molecular dynamics simulation. *Foods* 2021; **10(10)**, 2355.

[49] K Wang, Y Hong, Z Gu, L Cheng, Z Li and C Li. Stabilization of Pickering emulsions using starch nanocrystals treated with alkaline solution. *International Journal of Biological Macromolecules* 2020; **155**, 273-285.

[50] S Akbari and AH Nour. Emulsion types, stability mechanisms and rheology: A review. *International Journal of Innovative Research and Scientific Studies* 2018; **1(1)**, 11-17.